

# ELEVATED TEMPERATURE PROPERTIES OF A588 WEATHERING STEEL

FINAL REPORT

January 2014

Submitted by:

Maria Garlock

Associate Professor

Department of Civil and Environmental Engineering

Princeton University E330 EQuad

Princeton, NJ 08544

Jonathan Glsasman

Department of Civil and

Environmental Engineering

Princeton University

Samy Labbouz

Department of Civil and

Environmental Engineering

Princeton University

Submitted to:

Dave Lambert

New Jersey Department of Transportation

1035 Parkway Ave

Trenton, NJ 08618

In cooperation with

Rutgers, The State University of New Jersey

And

State of New Jersey

Department of Transportation

And

U.S. Department of Transportation

Federal Highway Administration

## **Disclaimer Statement**

The contents of this report reflect the views of the authors, who are responsible for the facts and the accuracy of the information presented herein. This document is disseminated under the sponsorship of the Department of Transportation, University Transportation Centers Program, in the interest of information exchange. The U.S. Government assumes no liability for the contents or use thereof.

The Center for Advanced Infrastructure and Transportation (CAIT) is a Tier I UTC Consortium led by Rutgers, The State University. Members of the consortium are the University of Delaware, Utah State University, Columbia University, New Jersey Institute of Technology, Princeton University, University of Texas at El Paso, University of Virginia and Virginia Polytechnic Institute. The Center is funded by the U.S. Department of Transportation.

1. Report No. <b>CAIT-UTC-021</b>		2. Government Accession No.		3. Recipient's Catalog No.	
4. Title and Subtitle <b>Elevated Temperature Properties of A588 Weathering Steel</b>			5. Report Date <b>January 2014</b>		
			6. Performing Organization Code <b>CAIT/Princeton University</b>		
7. Author(s) <b>Maria Garlock, Jonathan Glassman, Samy Labbouz</b>			8. Performing Organization Report No. <b>CAIT-UTC-021</b>		
9. Performing Organization Name and Address <b>Princeton University E330 EQuad Princeton, NJ 08544</b>			10. Work Unit No.		
			11. Contract or Grant No. <b>DTRT12-G-UTC16/ 155-6181</b>		
12. Sponsoring Agency Name and Address <b>Center for Advanced Infrastructure and Transportation Rutgers, The State University of New Jersey 100 Brett Road Piscataway, NJ 08854</b>			13. Type of Report and Period Covered <b>Final Report 2/1/13 –1/31/14</b>		
			14. Sponsoring Agency Code		
15. Supplementary Notes U.S. Department of Transportation/Research and Innovative Technology Administration 1200 New Jersey Avenue, SE Washington, DC 20590-0001					
16. Abstract In recent decades, bridge fires have become a major concern in the U.S. Fire hazard in bridges can result in significant economic and public losses. New construction of bridges often use “Weathering Steel” (also known as “Corten Steel”), which has a corrosion-retarding effect since the steel forms a protective rust layer on its surface under the influence of the weather. To date, no information exists on the high temperature mechanical properties of weathering steel. The objective of this work is to develop a database of mechanical properties of A588 weathering steel that has been exposed to high temperatures. These properties include the residual (after heating and cooling) stress-strain, fracture toughness, and surface hardness. The parameters that are investigated include temperature (800°F, 1000°F, 1200°F, and 1500°F), cooling methods (in air (CIA), and in water (CIW), representing fire-fighting effects), and material. Experiments are also done in a steady-state elevated temperature condition. A comparison is made between A588 weathering steel, used widely for bridges, and another material whose chemical composition and mechanical properties allows it to be classified by ASTM as both an older weathering steel (A242), a steel commonly used in building construction (A992), and also a non-weathering steel used for bridges (A709 Grade 50). The studies showed that at temperatures of 1200°F and below, the <i>residual</i> material properties of both materials studied (representing the post-fire condition), were affected no more than on the order of 10% compared to the unheated steel. Examining the residual properties of the CIW specimens, there is a clear trend of decreasing fracture toughness with increasing temperature. There is also a clear trend of increasing hardness with increasing temperature. It is expected that the CIW method produces different microstructure changes than the CIA method, thus resulting in the trends observed. Specimens tested to 1500°F showed a significant change in response, especially for the CIW method of cooling. At this temperature, it is likely that the steel has gone through a phase change. Practically speaking, a bridge that reaches 1500°F will experience significant permanent deformations if this temperature is widespread and in that case it will likely need to be demolished. Based on the results obtained thus far, it is likely that if significant permanent deformations are not observed, a bridge of A588 weathering steel has the potential to be put back into service following a fire.					
17. Key Words <b>fire, temperature, weathering steel, bridges</b>			18. Distribution Statement		
19. Security Classification (of this report) <b>Unclassified</b>		20. Security Classification (of this page) <b>Unclassified</b>		21. No. of Pages <b>35</b>	22. Price

## **Acknowledgments**

The assistance of James Ricles and Sougata Roy of Lehigh University throughout the development of this project is gratefully acknowledged. We also thank High Steel Inc. of Lancaster, PA for donating the A588 steel, and Lehigh University's ATLSS labs for donating the A992 steel. Carl Bowman, Instrumentation Manager of the ATLSS Engineering Research Center, and Joe Vocaturo, Senior Lab Manager of CEE at Princeton University provided invaluable support in the labs.

Finally, we thank CAIT who made this work possible. The patience and advice of Andres Roda is especially recognized.

## Table of Contents

1.0. DESCRIPTION OF THE PROBLEM .....	1
2.0. APPROACH AND OBJECTIVES .....	2
3.0. BACKGROUND.....	3
3.1. Weathering Steel .....	3
3.2. High Temperature Properties of Steel.....	3
4.0. METHODOLOGY: EXPERIMENTAL PROGRAM .....	4
4.1. Test Matrix .....	4
4.2. Steel Specimens .....	5
4.3. Heating and Cooling .....	7
4.4. ‘Hot’ Tension Tests.....	8
4.4.1. Specimen Preparation .....	10
4.4.2. Heating Procedure.....	10
4.4.3. Tensile Test Procedure.....	11
4.5. ‘Residual’ Tension Tests.....	11
4.6. Fracture Toughness .....	12
4.7. Hardness .....	13
5.0. FINDINGS OF EXPERIMENTAL RESULTS .....	14
5.1. Ambient Test Results (Control Group) .....	14
5.2. ‘Hot’ Tension Tests.....	15
5.3. ‘Residual’ Tension Tests.....	17
5.4. Fracture Toughness .....	20
5.5. Hardness.....	22
6.0. CONCLUSIONS .....	24
6.1. Effect of Temperature on Tensile Capacity .....	24
6.2. Effect of Cooling Method on Residual Mechanical Properties .....	24
6.3. Comparison of Materials.....	25
7.0. RECOMMENDATIONS .....	25
8.0. REFERENCES.....	26

## List of Figures

Figure 1. October 3, 2012 bridge fire, NJ Turnpike .....	2
Figure 2. Cross-section of I-195 bridge .....	2
Figure 3. Plots of (a) $k_{y,T}$ and $k_{p,T}$ versus temperature based on [30], and (b) stress-strain curves at 20°C, 400°C, 565°C, and 700°C, where the stress is normalized by $\sigma_y$ at ambient temperature, for the “fully nonlinear” material properties based on the Eurocode [30].....	4
Figure 4. Layout of specimens for Material 1.....	6
Figure 5. Layout of specimens for Material 2.....	6
Figure 6. ASTM E8 standard round tension test specimens used for the residual tests .....	6
Figure 7. ASTM E8 standard rectangular (flat) tension test specimens used for the hot tests in the furnace .....	6
Figure 8. ASTM E23 Type A impact test (CVN) specimens .....	6
Figure 9. (a) Heating and cooling test setup. (b) Furnace with three standard round specimens placed inside. The companion specimen is on the far right (with the thermocouple sticking out from one side), while the two specimens that will be mechanically tested after they have been heated and cooled are to the left of the companion specimen.....	8
Figure 10. (a) Companion specimen (with thermocouple inserted) along with two mechanical test specimens cooling in air on top of a ceramic blanket; (b) two mechanical specimens after being dunked in the water bath shown; (c) heat-resistant gloves and tongs used to remove the specimens from the furnace after heating.....	8
Figure 11. Furnace and tensile test frame setup at Lehigh University. A schematic of the setup is shown in Figure 9 .....	9
Figure 12. Spacing of furnace, cooling plates, and grips on the 30” and 36” long specimens. The copper plates (shown as yellow squares) cooled the steel specimen as it exited the furnace so that excess heat did not travel into the grips (shown as green trapezoids).....	9
Figure 13. Close up images of the cooling plates attached to the (a) bottom and (b) top of the specimen as it left the furnace. The cooling plates were made of copper with cold water continuously running through them to remove heat from the specimen before it reached the clamps .....	11
Figure 14. Ultimate tensile machine setup with standard round specimen and extensometer attached .....	12

Figure 15. CVN fracture hardness test.....	12
Figure 16. (a) Rockwell hardness machine setup, and (b) specimen placed beneath indenter...	13
Figure 17. Ambient tensile test results for Material 1 and Material 2 .....	14
Figure 18. Normalized ultimate stress versus temperature .....	15
Figure 19. Load-displacement curves for (a) Material 1 and (b) Material 2 (A588).....	16
Figure 20. Comparison of Materials 1 and 2 at (a) 800°F, (b)1000°F, (c)1200°F, (d)1500°F ...	16
Figure 21. Stress-strain relationships for few specimens of (a) <i>Material 1 CiA</i> (b) <i>Material 1 CiW</i> (c) <i>Material 2 CiA</i> and (d) <i>Material 2 CiW</i> at temperatures from 800 to 1500°F .....	17
Figure 22. Plots of average values of (a) $E$ , (b) $\sigma_y$ , and (c) $\sigma_u$ for Material 1 specimens that were heated to the temperature specified on the x-axis and cooled in air (CIA) or cooled in water (CIW). The ambient value is from the specimens that were not heated .....	19
Figure 23. Ductile and brittle failure of A242 test specimens .....	19
Figure 24. Plots of average values of (a) $E$ , (b) $\sigma_y$ , and (c) $\sigma_u$ for A588 steel specimens that were heated to the temperature specified on the x-axis and cooled in air (CIA) or cooled in water (CIW). The ambient value is from the specimens that were not heated .....	20
Figure 25. CVN energy for Material 1 specimens that were heated to the specified maximum temperature and cooled in water (open, red points) or cooled in air (solid, black points). Results from all tests for each temperature and cooling method are shown in (a); average values are plotted in (b) .....	21
Figure 26. CVN energy for specimens (A588 steel) that were heated to the specified maximum temperature and cooled in water (open, red points) or cooled in air (solid, black points). Results from all tests for each temperature and cooling method are shown in (a); average values are plotted in (b) .....	22
Figure 27. Rockwell hardness results for Material 1 .....	23
Figure 28. Rockwell hardness results for Material 2 (A588).....	23

## List of Tables

Table 1. Test matrix: Nomenclature of specimens and type of ASTM test performed .....	5
Table 2. Chemical analysis of materials tested and ASTM standards for various steels.....	7
Table 3. Summary of ambient temperature (unheated) test results .....	14
Table 4. Summary of ‘hot’ tension tests .....	15
Table 5. Residual tensile test results for Material 1 .....	18
Table 6. Residual tensile test results for Material 2.....	18
Table 7. Summary of fracture toughness (CVN) results.....	21
Table 8. Summary of Rockwell Hardness tests .....	23

## 1.0. DESCRIPTION OF THE PROBLEM

In recent decades, bridge fires have become a major concern in the U.S. [Garlock et. al 2012] Fire hazard in bridges can result in significant economic and public losses. Traffic on fire damaged bridges is usually hard to detour and can significantly affect traffic quality in the region. Further, a severe fire may result in permanent damage or even collapse of the bridge [Payá-Zaforteza and Garlock 2012]. While the perception may be that it is unlikely that a bridge will collapse under fire, a recent nationwide survey by the NYDOT has shown that nearly three times more bridges have collapsed due to fire than earthquakes [NYDOT 2008].

New construction of bridges often use “Weathering Steel” (also known as “Corten Steel”), which has a corrosion-retarding effect since the steel forms a protective rust layer on its surface under the influence of the weather. To date, no information exists on the high temperature mechanical properties of weathering steel. This research develops this knowledge for A588 weathering steel.

The motivating event for this work was a bridge fire that occurred on October 3, 2012. A dump truck traveling south on the NJ Turnpike crashed and caught fire under a bridge that carries I-195 over the Turnpike (Figure 1). This bridge was being widened and had timber shielding beneath it, which provided some protection for the steel from the intense heat of the fire. It was decided to not pursue any repairs since the bridge that was subject to fire was scheduled to be demolished in a few weeks and an adjacent replacement bridge was nearly complete. Instead, one of the I-195 west bound lanes was closed for precaution. This lane was reopened about a week later after a load test, with dump trucks, indicated that the fire-affected bridge had significant load capacity. [CAIT newsletter Jan. 2013].

The cross-section of the bridge is as shown in Figure 2. Girders G3 through G8 were part of the original bridge and made of A588 weathering steel Grade 50 [NJDOT 2010]. Girders G1 and G2 are the expansion to the bridge and based on the construction drawings they are of A709 Grade 50 (not weathering steel). The fire developed under G1, G2, and G3. This project examines the two types of steel that comprised this bridge. A588 weathering steel is the main focus of this study, and it is compared to another type of steel (which based on ASTM specifications can be classified as an older type of weathering steel (A242), A709, or A992) is examined as well. It was not possible to obtain the material of the actual I-195 bridge itself, so other material was procured as described in later sections.



**Figure 1.** October 3, 2012 bridge fire, NJ Turnpike.

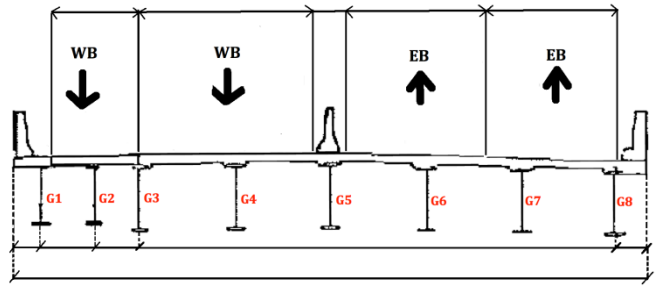


**Figure 2.** Cross-section of I-195 bridge.

## 2.0. APPROACH AND OBJECTIVES

The objective of this work is to develop a database of mechanical properties of A588 weathering steel that has been exposed to high temperatures. These properties include the residual (after heating and cooling) stress-strain, fracture toughness, and surface hardness. The parameters that are investigated include temperature and cooling methods.

The elevated temperature specimens will be heated to 427°C (800°F), 538°C (1000°F), 649°C (1200°F), and 815°C (1500°F). Two cooling methodologies are examined: cooling in air (CIA), and cooling in water (CIW). The latter represents firefighting effects. For the stress-strain tests, experiments will also be done in a steady-state elevated temperature condition. A comparison will be made between A588 weathering steel, used widely for bridges, and another material whose chemical composition and mechanical properties allows it to be classified by ASTM as both an older weathering steel (A242), a steel commonly used in building construction (A992), and a non-weathering steel used for bridges (A709 Grade 50).

There are two important reasons to know the high temperature properties of bridge steels: (a) to make a rapid post-fire assessment of a steel girder; and (b) to make informed decisions for potential heat straightening of bridge overpasses that have been affected by fire or have been impacted by a vehicle that exceeds the vertical clearance. This proposal is motivated by bridge fires, although the results can be applied to heat-straightening of impacted bridge girders as well.

Bridge fires, which result in extended congested detours to accommodate the time needed to assess and repair the bridge, affect the welfare of our transportation system. One of the long-term outcomes of this proposal will be to reduce the time for assessment and repair and possibly avoid needing to replace the bridge. This research therefore supports USDOT goals of ‘State of Good Repair’, which in turn supports making “... improvements to critical aspects of highway system performance (safety, congestion, reliability, infrastructure condition, air quality, user satisfaction, and emergency response)...”, and also ‘Economic Competiveness’, which addresses the negative impacts of congestion.

The outcomes from this research are data that can assist with rapid post-fire or post-impact assessment of weathering steel bridge girders. By knowing the residual mechanical properties at various temperatures, fast decisions can be made about repairing or replacing.

### **3.0. BACKGROUND**

#### **3.1. Weathering Steel**

As early as the 19th century, interest arose to develop a type of steel that would be resistant to corrosion. In the 1930s, the US Steel Corporation started developing their own low-alloy steels (containing copper, nickel, chromium, silicon and phosphorus for alloying elements), which from their alloying elements could demonstrate particularly good resistance to corrosion. USSC consequently derived the commercial name *Cor-Ten* for these steels, which stands for Corrosion-Resistance Tensile strength. [Wiss Janney 2013] By early 1940s, the American Society of Testing of Materials (ASTM) also conducted studies on low-alloy steels with enhanced corrosion resistance, essentially developing its first weathering steel, A242. [McDad et al. 2000]

More generally, weathering steels are high-strength low-alloy steels with particularly good corrosion resistance. This resistance comes from the capacity of the alloying element to form a tightly adhering patina, or rust layer, when oxidizing. The main difference between weathering steels and carbon steel is that this patina essentially acts as a protective layer for the steel, decreasing further corrosion rates. Corrosion of weathering steel can generally be divided into 3 distinct phases: initial rapid corrosion, decreasing corrosion rate and formation of protective layer and finally a stabilized phase, with linear loss of corrosion. [Kimura&Kihira 2005] It should be noted that the protective rust layer typically forms after 1 to 3 years of atmospheric exposure of the steel (depending on environmental conditions).

High resistance to corrosion and the consequent reduced life-cycle costs from rust-proof painting and maintenance have made weathering steels a popular choice for bridge construction in the US, with the first bridge built in 1964 in New Jersey. Weathering steels have since been increasingly employed in bridges, used today in 40-45% of new bridges built in the US, 90% in Canada, and hundreds of bridges throughout Europe and Japan. [AISI 1995]

#### **3.2. High Temperature Properties of Steel**

The Eurocode provides high temperature material properties of structural steel [CEN 2002]. Reduction factors for yield stress ( $\sigma_y$ ), proportional limit stress ( $\sigma_p$ ), and Young's modulus ( $E$ ) as a function of temperature are provided ( $k_{y,T}$ ,  $k_{p,T}$  and  $k_{E,T}$ , respectively). The Eurocode permits strain hardening for steel heated up to 400°C, and assumes that at 1200°C steel has lost all mechanical strength. Figure 3 provides plots for typical stress-strain curves based on Eurocode, where the assumption of yield stress is based on a strain of 0.02. Other models for estimating the high temperature properties of steel are available such as that by ASCE [Lie 1992] and NIST [Leuke et al. 2011].

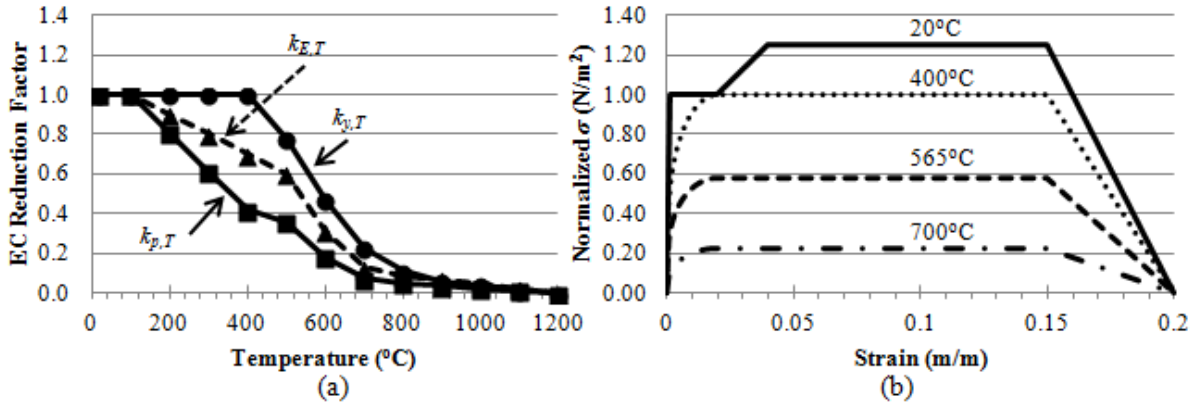


**Figure 3.** Plots of (a)  $k_{y,T}$ ,  $k_{p,T}$  and  $k_{E,T}$  versus temperature based on [30], and (b) stress-strain curves at 20°C, 400°C, 565°C, and 700°C, where the stress is normalized by  $\sigma_y$  at ambient temperature, for the “fully nonlinear” material properties based on the Eurocode [30].

The Pennsylvania Department of Transportation (PennDOT) conducted a study on A709 steel, which is typically used for bridges, to test its residual mechanical properties after being heated to 800°F and 1200°F [PennDOT 2011]. For their experiments, steel plates were heated using a jet flame. A thermocouple was installed during the heating to measure the specimen temperature. Tensile and CVN test coupons were cut from the steel as close to the flame impingement site as possible. Residual mechanical properties were measured, and it was reported that the fire exposures studied in this experiment (maximum steel temperature of 1200°F) had minimal effects on the residual yield strength, ultimate strength, and surface hardness. Slight reductions, however, were observed in CVN fracture toughness values. The researchers did not study temperatures exceeding 1200°F because they assumed that any steel member heated beyond this temperature and allowed to cool would have obvious physical deformations and would need to be replaced.

In addition to the residual mechanical properties tests, visual assessments were made of the steel test elements that had different coatings on them. The purpose of these tests was to develop a visual aid to help field engineers assess how much damage the bridge had sustained from a fire loading.

#### 4.0. METHODOLOGY: EXPERIMENTAL PROGRAM

##### 4.1. Test Matrix

The following parameters were studied: (1) Material, (2) Temperature; and (3) Cooling Method. Each parameter is discussed in detail below. Table 1 presents the test matrix, where the nomenclature for each test represents the following:

- **2** represents A588 weathering steel; **1** represents “Material 1,” which is classified as either A242, A992, or A709 based on ASTM chemical and mechanical material properties.

- **A** = ‘A’mbient temperature without having been previously heated. This represents the baseline case.
- **H** = the test is done with the specimen in the elevated temperature steady state (‘H’ot)
- **Ca** = the specimen is tested after it has been ‘C’ooled in the ‘a’ir
- **Cw** = the specimen is tested after it has been ‘C’ooled in ‘w’ater
- The last numbers represent the target maximum temperature (in Fahrenheit) to which the specimen was heated.

**Table 1.** Test matrix: Nomenclature of specimens and type of ASTM test performed\*\*

Temp. during <sub>fact</sub>	Material *	Cooling	Maximum steady state temperature				
			70 F (20C)	800 F (538 C)	1000 F (538 C)	1200 F (649 C)	1500 F (815 C)
<b>Hot</b>	<b>1</b>	--	1A (E8, E23, E18)	1H-800 (E8)	1H-1000 (E8)	1H-1200 (E8)	1H-1500 (E8)
	<b>2</b>		2A (E8, E23, E18)	2H-800 (E8)	2H-1000 (E8)	2H-1200 (E8)	2H-1500 (E8)
<b>Cooled (Residual)</b>	<b>1</b>	<b>air</b>	-	1Ca-800 (E8, E23, E18)	1Ca-1000 (E8, E23, E18)	1Ca-1200 (E8, E23, E18)	1Ca-1500 (E8, E23, E18)
	<b>2</b>		-	2Ca-800 (E8, E23, E18)	2Ca-1000 (E8, E23, E18)	2Ca-1200 (E8, E23, E18)	2Ca-1500 (E8, E23, E18)
	<b>1</b>	<b>water</b>	-	1Cw-800 (E8, E23, E18)	1Cw-1000 (E8, E23, E18)	1Cw-1200 (E8, E23, E18)	1Cw-1500 (E8, E23, E18)
	<b>2</b>		-	2Cw-800 (E8, E23, E18)	2Cw-1000 (E8, E23, E18)	2Cw-1200 (E8, E23, E18)	2Cw-1500 (E8, E23, E18)

\* 1 = Material 1 = A242, A992, A709; 2 = Material 2 = A588 weathering steel

\*\* E8 = tensile tests; E23 = Charpy V-notch fracture toughness tests; E18 = Rockwell surface hardness

As a baseline, specimens were tested at ambient temperature. A comparison of the results of ambient tests with tests at elevated temperature will help to establish the effect of elevated temperature on the mechanical properties. The elevated temperature specimens will be (1) heated to 427 °C (800 °F), 538 °C (1000 °F), 649 °C (1200 °F), and 815 °C (1500 °F), (2) held at that temperature to reach steady state condition throughout the specimen, and (3) cooled using one of two methods discussed next. These temperatures represent a variety of potential steel temperatures in a fire event. In addition, another set of uniaxial tension tests were done during the heated steady state condition of the temperatures listed above.

## 4.2. Steel Specimens

The steel specimens were cut from Material 1 as shown in Figure 4, and from Material 2 (A588) as shown in Figure 5. Figure 6 shows the ASTM E8 standard round tension test specimens used for the residual tests. Figure 7 shows the ASTM E8 standard rectangular (flat) tension test specimens used for the hot tests in the furnace. Figure 8 shows the ASTM E23 Type A impact test (CVN) specimens.

Laboratory Testing Inc. performed a chemical analysis of the material tested (direct reading atom emissions spectroscopy). The results are shown in Table 2 in addition to the ASTM chemical requirements for various steels.

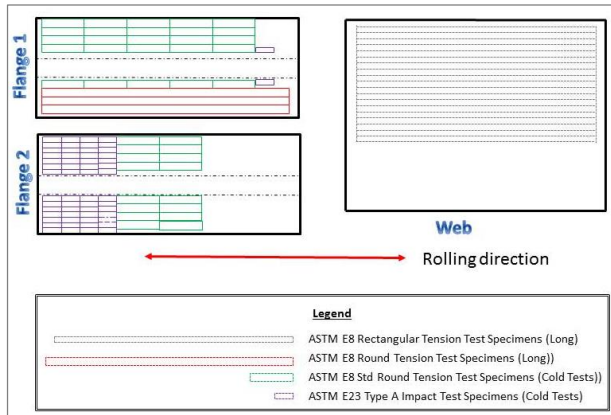


Figure 4. Layout of specimens for Material 1.

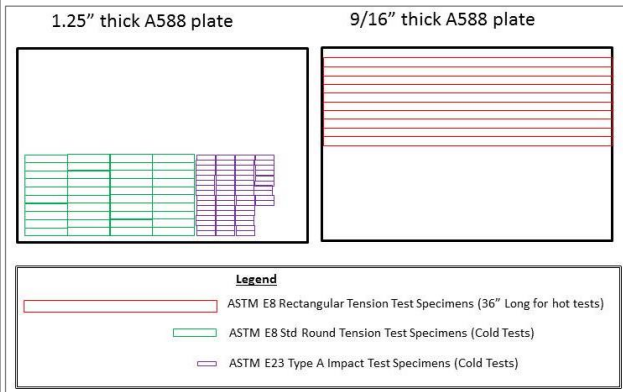


Figure 5. Layout of specimens for Material 2.

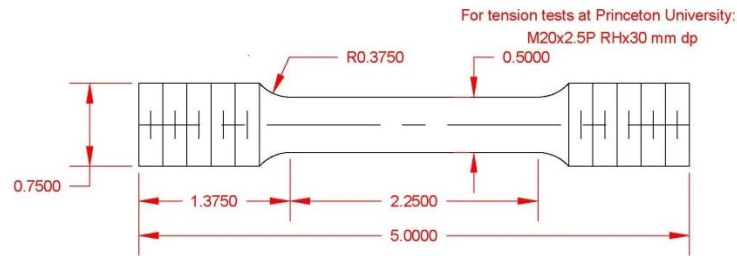


Figure 6. ASTM E8 standard round tension test specimens used for the residual tests (inches).

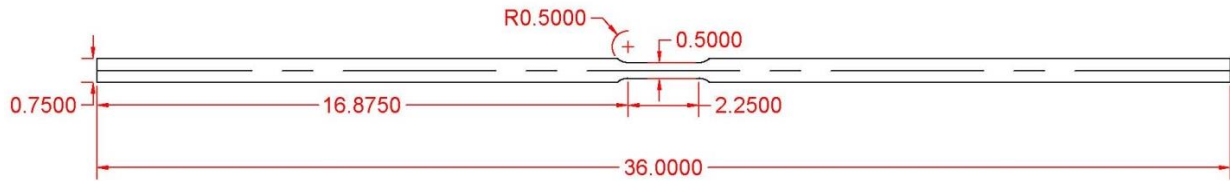


Figure 7. ASTM E8 standard rectangular (flat) tension test specimens used for the hot tests in the furnace (inches).

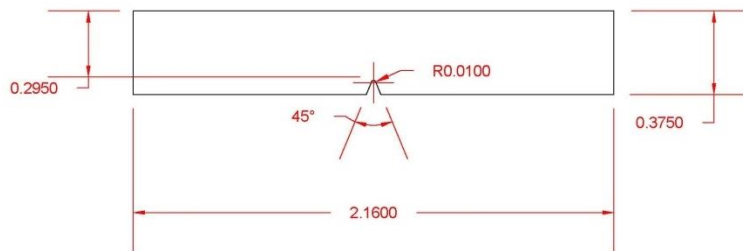


Figure 8. ASTM E23 Type A impact test (CVN) specimens (inches).

**Table 2.** Chemical analysis of materials tested and ASTM standards for various steels.

		Material 1	Material 2		ASTM A992 (2011)	ASTM A242 (1979)	ASTM A709 (2013)	ASTM A588 (2010)	
Element		W36x160	9/16" Plate	1-1/4" Plate		Type 2	Grade 50	Grade A	Grade B
Aluminum	Al	0.001	0.015	0.03					
Boron	B	0.0009	0.0012	0.0005					
Carbon	C	0.086	0.11	0.17	0.25 max	0.2 max	0.23 max	0.19 max	0.20 max
Cobalt	Co	0.007	0.005	0.006					
Chromium	Cr	0.085	0.51	0.48	0.35 max			0.40 - 0.65	0.40 - 0.70
Copper	Cu	0.255	0.29	0.3	0.60 max	0.2 max	0.20 min	0.25 - 0.40	0.20 - 0.40
Manganese	Mn	1.06	0.83	1.03	0.5 - 1.6	1.35 max	1.35 max	0.80 - 1.25	0.75 - 1.35
Molybdenum	Mo	0.03	0.031	0.016	0.15 max			-	-
Niobium *	Nb	0.011	<0.001	<0.001	0.05 max		0.005 - 0.05	-	-
Nitrogen	N								
Nickel	Ni	0.12	0.15	0.22	0.45 max			0.40 max	0.50 max
Phosphorus	P	0.014	0.01	0.01	0.035 max	0.04 max	0.04 max	0.04 max	0.04 max
Sulfur	S	0.017	0.03	0.01	0.045 max	0.05 max	0.05 max	0.05 max	0.05 max
Silicon	Si	0.19	0.38	0.32	0.40 max		0.40 max	0.30 - 0.65	0.15 - 0.50
Tin	Sn	0.011	0.012	0.011					
Thallium	Tl	0.001	0.001	0.001					
Vanadium	V	0.012	0.03	0.03	0.15 max		0.06 max	0.02 - 0.10	0.01 - 0.10

### 4.3. Heating and Cooling

In order to determine the ‘residual’ mechanical properties (Young’s modulus, yield and ultimate stress, fracture toughness, and surface hardness), the standard round and the CVN the specimens were heated using a Barbstead Thermolyne 6000 electric furnace at Princeton University. The furnace was set to the target temperature (800°F, 1000°F, 1200°F, and 1500°F) and the specimen was left in the furnace until its internal temperature reached the target temperature.

To ensure the standard round and CVN test specimens had reached the target temperature, a companion specimen was fabricated that was heated alongside the test specimens used to determine the residual mechanical properties. The companion specimen, shown in Figure 6 alongside its mechanical test specimen, had a 1/16” diameter hole drilled longitudinally from one end of the specimen to the center of the gauge length. An Omega TJ48-CAXL-116U-60 high temperature resistant thermocouple was inserted into this drilled hole to track the internal temperature of the companion specimen. This particular thermocouple was selected since it could handle the high temperatures of the experiment (up to 1500°F) and could also be placed in water to track how the steel cooled when dunked in water. Temperature data was read using an Iotech personal daq (data acquisition) along with the DaisyLab 7.0 software. Additional wired thermocouples were used to measure the ambient air temperature of the lab, which was important information for the specimens that were cooled in air. The entire setup (furnace, data acquisition system, thermocouple, water bath, and ceramic blanket) is shown in Figure 9(a).



**Figure 9.** (a) Heating and cooling test setup. (b) Furnace with three standard round specimens placed inside. The companion specimen is on the far right (with the thermocouple sticking out from one side), while the two specimens that will be mechanically tested after they have been heated and cooled are to the left of the companion specimen.

Both the companion and mechanical test specimens were placed close together in the furnace (see Figure 9(b)) such that the temperatures of the companion and mechanical test specimens could be safely interpreted to be the same. Once the target temperature was recorded by the thermocouple, a hold of at least 10 minutes was maintained to ensure uniformity and stability of the specimen temperatures. Following this 10 minute hold, the test specimens and companion specimen (with thermocouple still attached) were removed from the furnace and either placed on a ceramic blanket (for the CIA test) or immediately dunked in water (for the CIW test). The thermocouple remained inside the companion specimen at all times to track the cooling rate. Figure 10(a) shows the test and companion specimens cooling on top of a ceramic blanket (CIA), while Figure 10(b) shows the test and companion specimens after they have been dunked in water. Two people were typically present to remove the test and companion specimens from the furnace using tongs and heat-resistant gloves (shown in Figure 10(c)).



**Figure 10.** (a) Companion specimen (with thermocouple inserted) along with two mechanical test specimens cooling in air on top of a ceramic blanket; (b) two mechanical specimens after being dunked in the water bath shown; (c) heat-resistant gloves and tongs used to remove the specimens from the furnace after heating.

#### 4.4. ‘Hot’ Tension Tests

Tensile strength of both materials were investigated at high temperature. The specimens were placed in a SATEC furnace, and could be tested in tension while being heated by the furnace. Setup is illustrated in Figures 11 and 12. These tests, conducted at Lehigh University, used “long” steel specimens to accommodate for the dimension of the furnace and tensile testing equipment. The Material 1 “long” specimens were 30 inches long, and the A588 were 36 inches long.

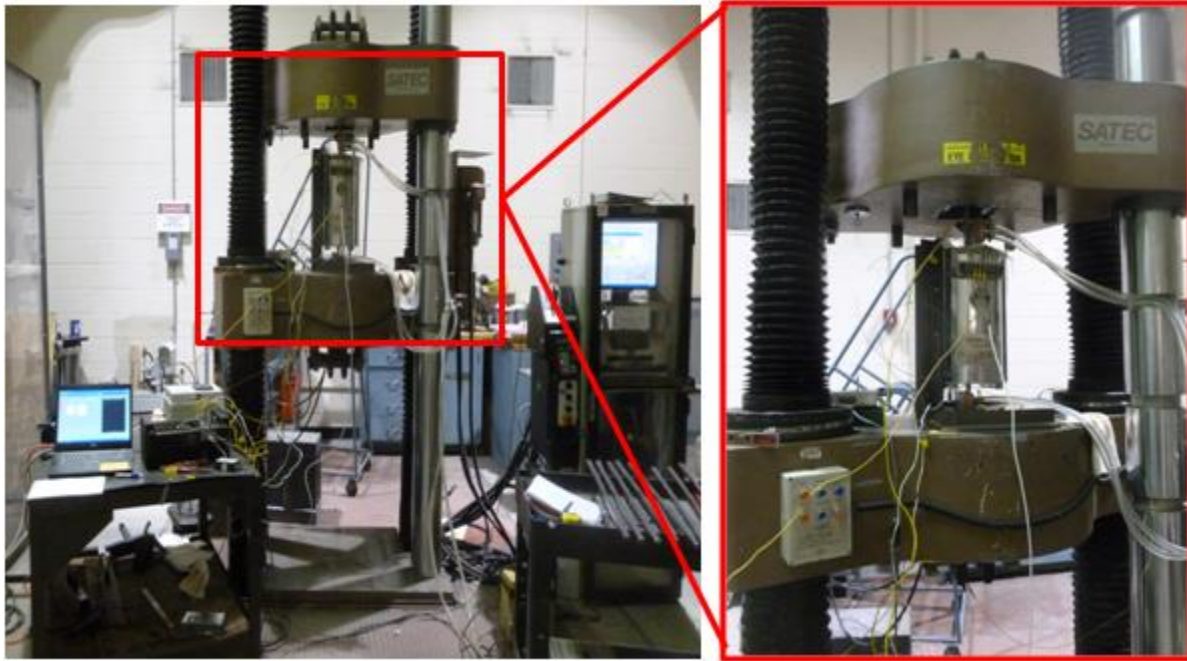


**Figure 11.** Furnace and tensile test frame setup at Lehigh University. A schematic of the setup is shown in Figure 9.

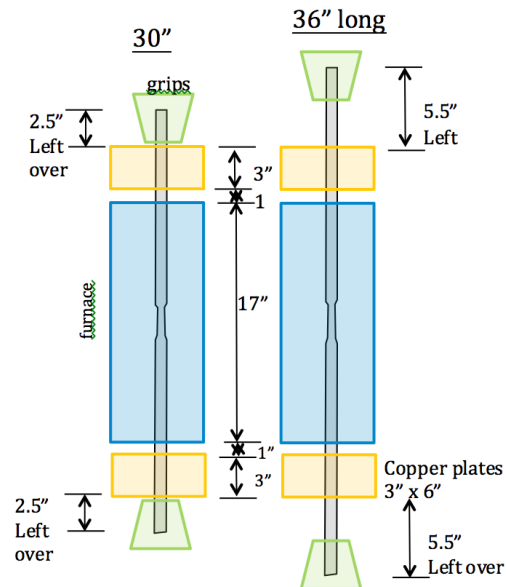


**Figure 12.** Spacing of furnace, cooling plates, and grips on the 30'' and 36'' long specimens. The copper plates (shown as yellow squares) cooled the steel specimen as it exited the furnace so that excess heat did not travel into the grips (shown as green trapezoids).

In addition to the furnace, the experimental apparatus consisted of SATEC tension machine, high temperature resistant thermocouples (Omega TJ48-CAXL-116U-60), and cooling clamps. The latter consisted of copper plates clamped to the specimen, through which cold water was continuously running, and that ensured the temperature at the grip location would remain sufficiently cool to not compromise the tensile testing procedure (see Figure 12).

The temperature in the furnace and during the whole test procedure was continuously monitored using several high temperature resistant thermocouples. The location of these thermocouples depended on the length of the specimens, and consequently the space available on the surface to place the thermocouples. However, in all high temperature tests, at least 4 thermocouples were used: one at each end of the gage length and one outside of each cooling plate. High temperature resistant thermocouples were used at the gauge location, and wire thermocouples were used where relatively cool temperature expected (due to their rubber casing, could not withstand very high temperatures)

Overall, the experimental procedure can be divided into three main sections: specimen preparation, specimen heating, and finally tensile test as described in the following sections.

#### *4.4.1. Specimen Preparation*

In order to test the steel specimens in the apparatus described above, a few preparations were necessary. First, the thermocouples had to be attached on the surface of the steel. This was done by welding a thin sheet of metal that would fix the tip of the thermocouple tightly against the surface. To apply this weld effectively, the surface of the specimen had to be cleaned with an electric sander at these locations.

All the specimens were also punch-marked at both ends with a number to keep track of them after rupture, as well as marked with two punches distant 2" in the gage length. Width and thickness were measured at each of the punch mark locations, as well as in mid-gage, and were used to determine average cross-sectional area. The distance between punch marks was exactly measured using a Starrett 799 electronic caliper, and will be used to estimate the amount of strain during test.

#### *4.4.2. Heating Procedure*

Once prepared, the specimen was placed inside the furnace and testing apparatus (see Figure 13). Note that during the heating procedure, only the bottom clamps were attached (free to elongate at top). An insulating blanket was placed above the furnace to minimize heat losses and protect equipment from rising heat, and the cooling plates attached above and below the furnace. While we tried to maximize the length of the specimen that was placed in the grips, a minimum length within the grips of 2" was maintained for the 30" long specimens; a 3" minimum was maintained for the 36" long specimens.

Before turning on the furnace, a health check of all thermocouple readings was done by making sure they all were consistent in their ambient temperature readings. Once the goal temperature was reached the specimen was left at constant temperature for at least 20 minutes before the tensile test would start. This was to ensure temperature equilibration inside the furnace and throughout the steel specimen.



**Figure 13.** Close up images of the cooling plates attached to the (a) bottom and (b) top of the specimen as it left the furnace. The cooling plates were made of copper with cold water continuously running through them to remove heat from the specimen before it reached the clamps.

#### 4.4.3. Tensile Test Procedure

After the specimen was left to equilibrate at the desired temperature for a minimum of 20 minutes, the tensile test procedure started. The first step was to close the top clamp (that had been left unclamped during the heating process to allow thermal elongation), which resulted in a compression force of about 2000 lbs. Therefore, before starting every test, it was necessary to zero this load by moving slightly the table position, relieving this compressive stress.

A final consideration was that the measure of head travel would not be an accurate representation of the steel extension due to seating in the machine. To correct this, we used a string potentiometer, attached to the traveling head, which would be a more accurate measure of total specimen elongation during test. A constant strain rate of 0.1 in/min was used in the tests.

#### 4.5. ‘Residual’ Tension Tests

Residual tensile strength tests were done for standard round specimens that were heated to 800°F, 1000°F, 1200°F, and 1500°F, and were subsequently cooled in air (CIA) or cooled in water (CIW). These tensile tests conformed to ASTM E8 and were conducted at Princeton University using an Instron 600 DX loading frame with a 600 kN load capacity, shown in Figure 14. An extensometer was used to measure strain during the initial portion of the tensile test. This extensometer was removed well before ultimate tensile strength was reached to avoid damaging the extensometer at fracture, but after yield was reached in all cases. The loading rate specified for the tensile test was 0.1 in/min, which was the same loading rate used for the hot tension tests at Lehigh University based on ASTM E8 guidelines.

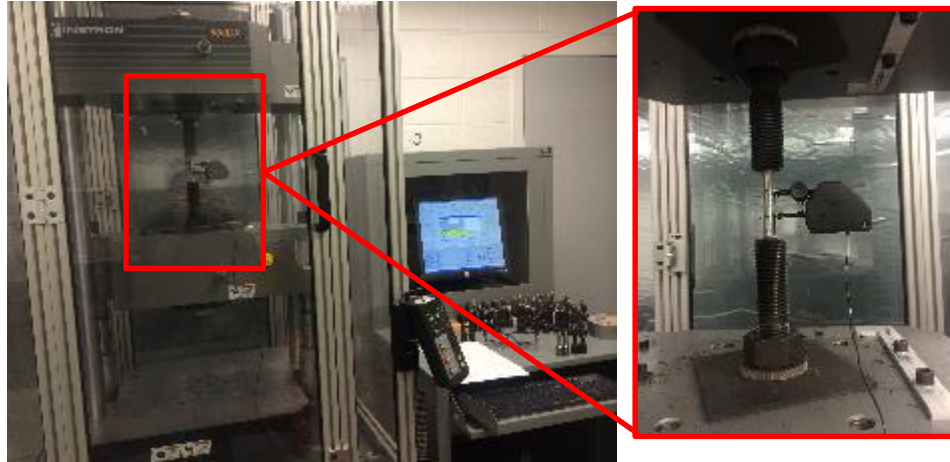


**Figure 14.** Ultimate tensile machine setup with standard round specimen and extensometer attached.

#### 4.6. Fracture Toughness

Charpy V-notch tests were conducted according to ASTM E23/AASHTO T266 guidelines. Lehigh University provided the impact test machine for these tests. Figure 15 shows an image of the instrument and the specimen setup.

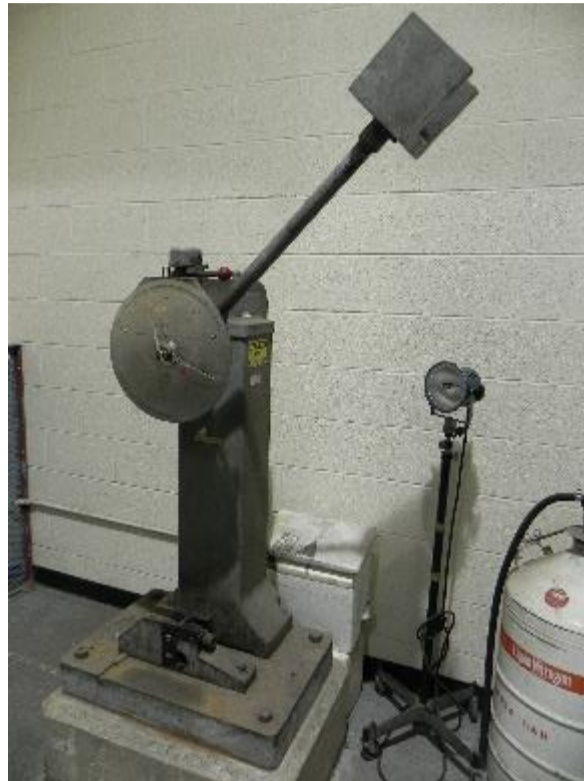


**Figure 15.** CVN fracture hardness test.

## 4.7. Hardness

The Rockwell hardness test provides a measure of the resistance of a metal to permanent indentation. This is done by measuring the additional depth to which an indenter is forced by a load beyond the depth of previously applied light load (pre-load) [Wilson Instruments]. We used the CVN specimens previously tested for toughness to conduct these hardness tests per ASTM E18.

Different scales can be used to measure hardness. For steel and hard metals, Rockwell Hardness Scales B or C are commonly preferred. The former, HRB, uses a 1/16" steel ball as indenter and a 100kgf test force, whereas HRC uses a spheroconical diamond indenter and a 150 kgf test load. The pre-load was 10 kgf in both cases, in accordance with ASTM stipulations. The details of the procedure can be covered by ASTM E18/AASHTO T80.

We used HRB in all of our tests, except in one case where the cooled metal was too hard, and had to use HRC, and used a Hardness testing machine Mitutoyo ATK-600.

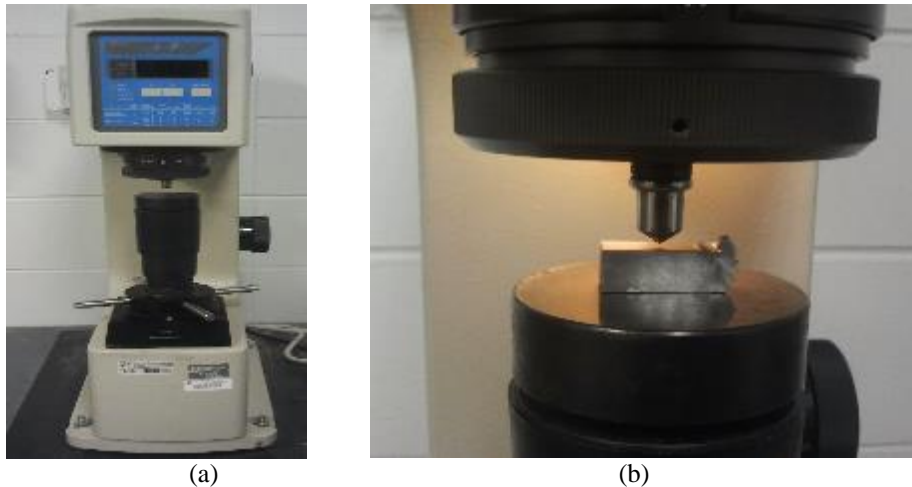


**Figure 16.** (a) Rockwell hardness machine setup, and (b) specimen placed beneath the indenter.

According to ASTM E-18 testing procedure recommendations, a daily verification of the digital hardness reading should be performed using a standard test block. Since we conducted all the hardness tests in one day, we performed this verification once for before starting the HRB procedure, and once before using HRC. Both verifications were successful, with hardness readings falling in the specified tolerances.

After these initial verifications, the specimen could be placed on the flat anvil. The indenter was then brought into contact with the steel, and the pre-force applied (this is achieved when a reading of 360 to 370 is obtained on digital monitor, c.f. Mitutoyo). Force was then increased and the hardness reading was obtained.

According to ASTM-E18, several conditions had to be met before testing. A room temperature of 50-95°F, but also a minimum steel specimen thickness of 10 times expected indentation depth should be used (for HRC, minimum of 0.04 in specified as approximation). Finally to ensure

accurate test results, the distance from center of indentation to edge of specimen must be at least 2.5 diameters and distance between two consecutive indentations must be at least 3 diameters.

## 5.0. FINDINGS OF EXPERIMENTAL RESULTS

The experimental results are presented in this section. A discussion of the effects of the parameters studied is presented in Section 5.0.

### 5.1. Ambient Test Results (Control Group)

A summary of the ambient test results are presented in Table 3 where  $\sigma_y$  is the yield stress,  $\sigma_u$  is the ultimate stress, and E is the modulus of elasticity. These results are what will be used for comparison and represent the ‘control group’. It is seen that both materials have similar properties at ambient except that Material 1 has a larger fracture toughness (as represented by the CVN tests) and smaller  $\sigma_u$  than A588. Figure 17 shows the tensile test results for the two materials.

**Table 3.** Summary of ambient temperature (unheated) test results.

Specimen	Tensile tests			CVN Tests		Rockwell B Tests	
	$\sigma_y$ (ksi) avg.	$\sigma_u$ (ksi) avg.	E (ksi) avg.	(ft-lb) avg.	std. dev	hardness avg.	std. dev
Material 1(1A)	59.0	71.0	28930	183	20	80.7	0.6
Material 2 (A588) (2A)	58.7	84.8	27760	125	10	86.1	0.4

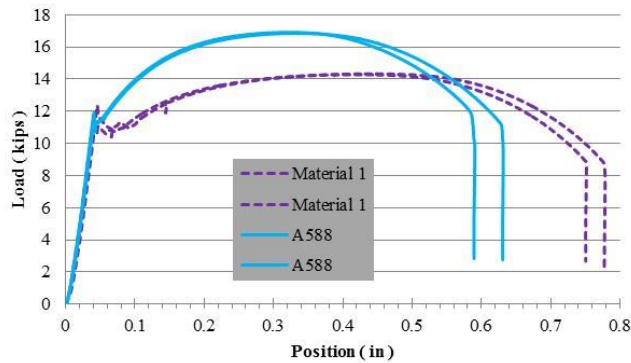


**Figure 17.** Ambient tensile test results for Material 1 and Material 2.

## 5.2. ‘Hot’ Tension Tests

Table 4 presents  $\sigma_u$  for the tensile tests that were done while the specimen was heated to the target temperature. Figure 18 plots  $\sigma_u$  normalized by the ambient stress value. It is seen that, as expected,  $\sigma_u$  decreases with increasing temperature. Also, the A588 steel loses strength faster at elevated temperatures than Material 1.

For highly nonlinear materials, the yield stress ( $\sigma_y$ ) is typically measured by the 0.2% offset method. Due to set up constraints, we were not able to measure strain directly (an extensometer could not be placed in the furnace). The string pot located outside the furnace provides some indication of yield, but until we can analyze the specimens further to show that all elongation occurred in the gage length, we cannot report the yield stress values for elevated temperatures.

**Table 4.** Summary of ‘hot’ tension tests.

	Spec.	$\sigma_u$ (ksi)		
		each	avg	ratio*
Material 1	1A	70.7 71.3	71.0	--
	1H-800	70.8 67.1	69.0	0.97
	1H-1000	43.6 44.7	44.1	0.62
	1H-1200	23.7 23.7	23.7	0.33
	1H-1500	9.1 8.3	8.7	0.12
Material 2 (A588)	2A	84.8 84.8	84.8	--
	2H-800	60.8 63	61.9	0.73
	2H-1000	42.8 42.1	42.4	0.50
	2H-1200	- 21.1	21.1	0.25
	2H-1500	7.8 8.0	7.9	0.09

\* ratio = the average value of the 1H or 2H specimens divided by the average value of Specimen 1A or 2A.

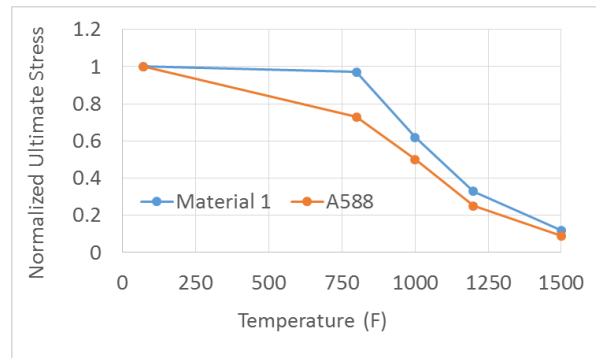


**Figure 18.** Normalized ultimate stress versus temperature

Figure 19 plots the load-displacement curves of the heated specimens for Material 1 and Material 2 (A588). For Material 1, all the specimens presented in these figures were the flat 30 inch long specimens. Material 2 used 36 inch long specimens (Fig.7) except for the ambient temperature tests (2A), which were the standard 5-inch long round specimens (Fig. 6). Note that data for the two 1H-1200 specimens has had to be corrected due to initial pre-compression due to closing of the clamps. Also, it can be seen from Figure 19 that one curve for 2H-1200 is off from the origin of the plot. This is because for this particular specimen the initial pre-compression applied by clamping was not zeroed. For this reason, results for this specimen were omitted from Table 4.

Overall, it is observed that the pairs of specimens give similar results thus indicating that two specimens per temperature is sufficient.

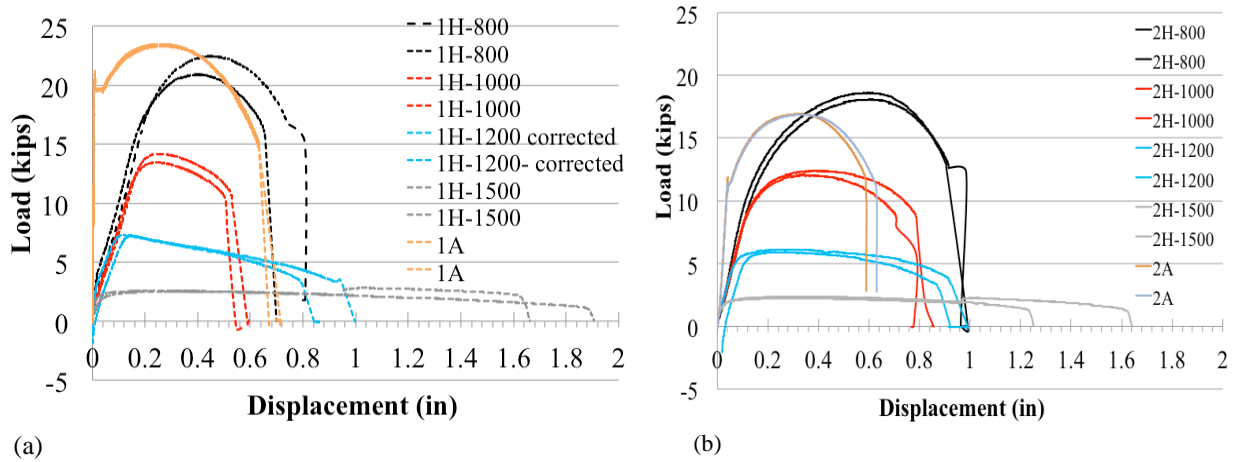


Figure 19. Load-displacement curves for (a)Material 1, and (b) A588

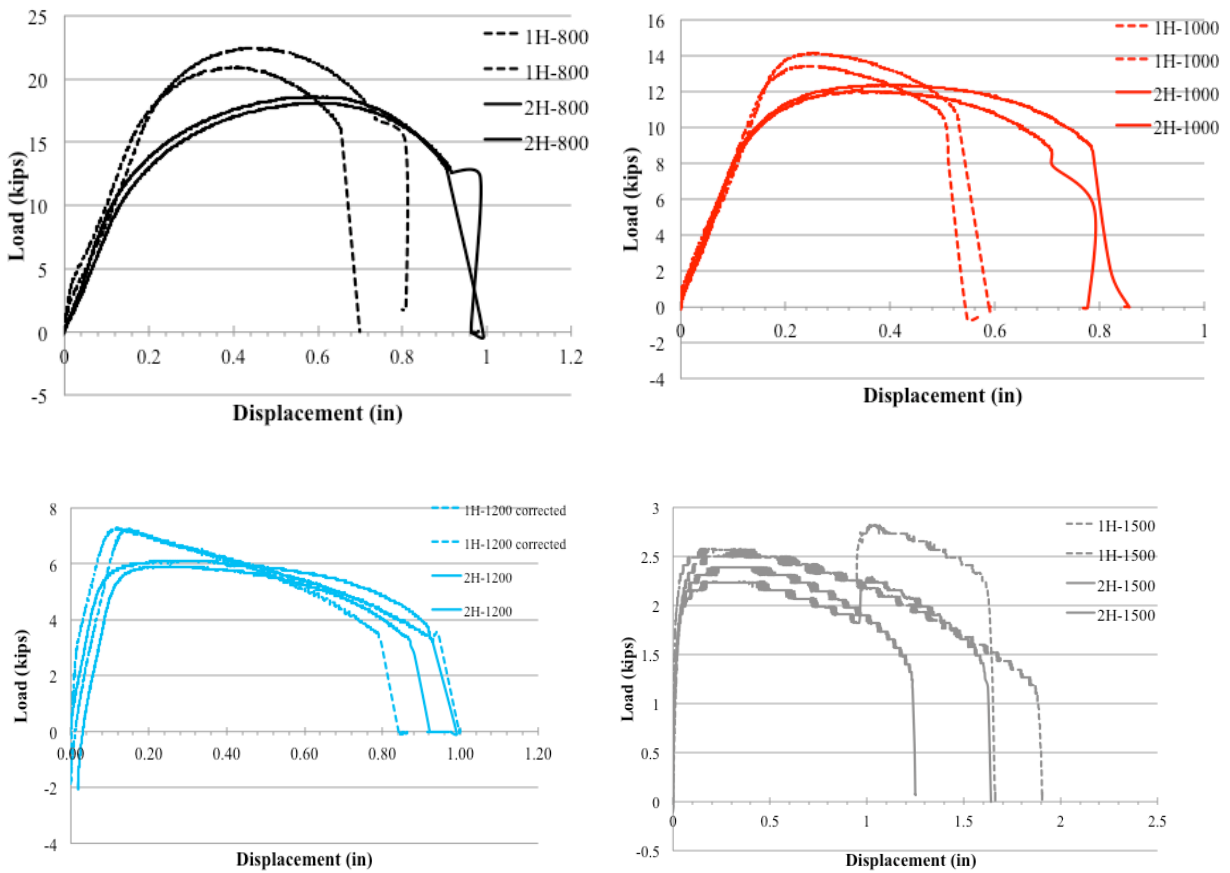
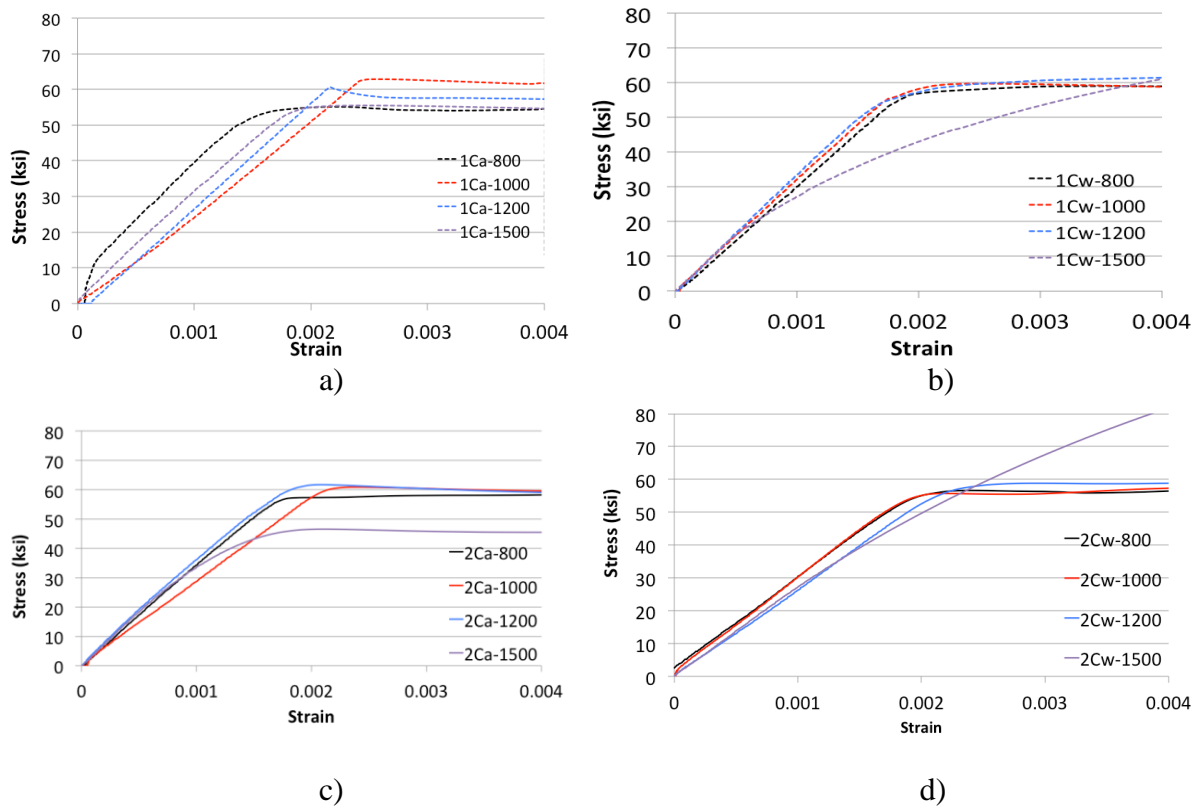


Figure 20. Comparison of Materials 1 and 2 (A588) at (a) 800°F, (b) 1000°F, (c) 1200°F, (d) 1500°F.

In addition to observing the difference in tensile test results with increasing temperature it is interesting to compare the load-displacement behavior at a given temperature between the two different steels studied in this report. In Figure 20, for the 1500°F tests, some unusual jumps in the stress-strain curves can be observed. These were caused by a change in the strain rate that was programmed into the controller software without the researchers being aware of it. In the software used to control the tensile test, a strain rate of 0.1 in/min was set until 1” total displacement was measured. After this amount of head travel, the software automatically changed strain rate to 0.5 in/min. Unknowingly, the strain rate changed during two of the four 1500°F tests (1H-1500A, 2H-1500).

### 5.3. ‘Residual’ Tension Tests

Two standard round specimens were tested for each CIA and CIW specimen (see Table 1). Tables 5 and 6 summarize the results for these specimens (for Material 1 and 2, respectively), which represent the residual strength of the material after being heated and cooled. The yield 0.2% offset method was used to calculate the yield stress ( $\sigma_y$ ) for all specimens. Figure 21 shows the stress-strain curves for some of the residual tension strength tests. The strains were measured using the extensometer, which needed to be removed after yield to protect it from falling off the specimen and breaking.



**Figure 21.** Stress-strain relationships for few specimens of (a) *Material 1 CiA* (b) *Material 1 CiW* (c) *Material 2 (A588) CiA* and (d) *Material 2 (A588) CiW* at temperatures varying from 800 to 1500°F.

**Table 5.** Residual tensile test results for Material 1.

Spec.	$\sigma_y$ (ksi)			$\sigma_u$ (ksi)			E (ksi)			
	each	avg	ratio*	each	avg	ratio*	each	avg	ratio*	
<b>1A</b>	<b>56.1</b> <b>54.9</b>	<b>55.5</b>	--	<b>70.7</b> <b>71.3</b>	<b>71.0</b>	--	<b>26100</b> <b>31770</b>	<b>28930</b>	--	
CIA	1Ca-800	54.2 57.4	55.8	1.01	68.7 72.2	70.5	0.99	31820 32680	32250	1.11
	1Ca -1000	56.7 61.7	59.2	1.07	71.9 72.6	72.3	1.02	26260 26860	26560	0.92
	1Ca -1200	54.8 57.4	56.1	1.01	70.8 71.1	70.9	1.00	32860 29640	31250	1.08
	1Ca -1500	54.7 48.8	51.8	0.93	71.2 70.2	70.7	1.00	29260 27240	28250	0.98
CIW	1Cw-800	59.0 59.7	59.4	1.07	72.9 72.8	72.8	1.03	31000 28170	29590	1.02
	1Cw-1000	59.2 56.2	57.7	1.04	74.5 74.1	74.3	1.05	32060 33610	32840	1.13
	1Cw-1200	60.7 61.3	61.0	1.10	78.5 77.3	77.9	1.10	34600 33280	33940	1.17
	1Cw-1500	59.8 68.8	64.3	1.16	114.0 109.9	111.9	1.58	24010 25860	29940	1.03

\* ratio = the average value of the CIA or CIW specimens divided by the average value of Specimen 1A.

**Table 6.** Residual tensile test results for Material 2.

Spec.	$\sigma_y$ (ksi)			$\sigma_u$ (ksi)			E (ksi)			
	each	avg	ratio*	each	avg	ratio*	each	avg	ratio*	
<b>2A</b>	<b>56.7</b> <b>56.9</b>	<b>56.8</b>	--	<b>84.8</b> <b>84.8</b>	<b>84.8</b>	--	<b>30040</b> <b>25480</b>	<b>27760</b>	--	
CIA	2Ca-800	58.0 57.1	57.6	1.01	85.4 84.2	84.8	1.00	33700 37830	35770	1.29
	2Ca -1000	59.1 59.5	59.3	1.04	84.4 86.1	85.2	1.00	30970 28490	29730	1.07
	2Ca -1200	59.2 59.2	59.2	1.04	83.6 83.5	83.5	0.99	26540 33970	30260	1.09
	2Ca -1500	45.6 44.7	45.1	0.79	79.6 79.2	79.4	0.94	34760 26270	30520	1.10
CIW	2Cw-800	56.7 56.4	56.6	1.00	85.9 85.7	85.8	1.01	35050 27920	31490	1.13
	2Cw-1000	57.5 57.3	57.4	1.01	87.2 86.0	86.6	1.02	30440 29070	29760	1.07
	2Cw-1200	58.7 59.0	58.9	1.04	87.4 87.1	87.3	1.03	25260 26770	26020	0.94
	2Cw-1500	102.4 89.7	96.1	1.69	160.8 157.5	159.1	1.88	27330 30750	29040	1.05

\* ratio = the average value of the CIA or CIW specimens divided by the average value of Specimen 2A.

Figure 22 plots the average results for Material 1 steel specimens normalized by the control values (specimens that were never heated). From Table 5 and Figure 22(a) it is observed that for both cooled in water (CIW) and CIA specimens,  $\sigma_y$  typically stays within 10% of the control value, except for the CIW specimens heated to 1500°F. The same is observed for  $\sigma_u$  in Figure 22(b) with one major exception: the CIW specimens at 1500°F experience a 58% increase in value. The residual  $E$  value is plotted in Figure 22(c) and it is shown that the CIA specimens generally fluctuate within 10% of the control value, but the CIW values all tend to be larger than the control value and for CIW at 1200°F  $E$  exceeds the control by 17%.

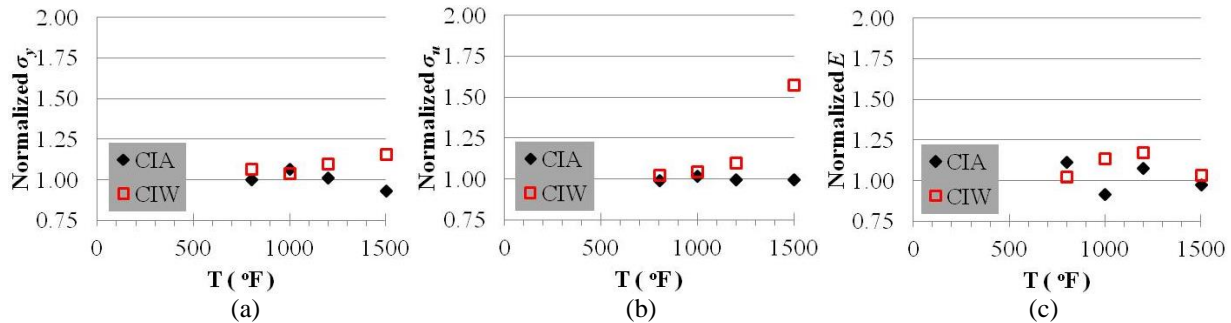


**Figure 22.** Normalized plots of average values of (a)  $\sigma_y$ , (b)  $\sigma_u$ , and (c)  $E$  for Material 1 specimens that were heated to the temperature specified on the x-axis and cooled in air (CIA) or cooled in water (CIW). The normalization is based on the average ‘control’ value from the specimens that were not heated.

Another general observation of these experiments is that for Material 1, brittle failure was observed for the CIW specimens that were heated to 1500°F. Figure 23 compares the image of the control (1A) specimen to the CIW specimen heated to 1500°F. The lack of ‘necking’ in the CIW specimen on the right is a visual representation of the brittle nature of the material.



**Figure 23.** Ductile and brittle failure of Material 1 test specimens. Ductile failure is shown on the left for specimen 1A (unheated) compared to brittle failure observed on the right for specimen 1Cw-1500.

Figure 24 plots the average results for A588 steel specimens normalized by the control values (specimens that were never heated). From Figure 24(a), it is seen that for temperatures up to 1200°F,  $\sigma_y$  does not differ significantly compared to the control value regardless of cooling

method. At 1500°F however, the CIA specimens only retain 79% of  $\sigma_y$  and the CIW specimens have a 69% increase in  $\sigma_y$ . Figure 24(b) shows that  $\sigma_u$  is hardly affected when the CIA method is used. The same is observed for the CIW method except for 1500°F where an 88% increase in  $\sigma_u$  is observed. Figure 24(c) shows that the CIA specimens experienced an increase in  $E$  values on the order of 10% except for the 800°F specimen where  $E$  increased 29%. The CIW specimens had residual  $E$  values that were generally within 10% (above or below) of the control specimen value.

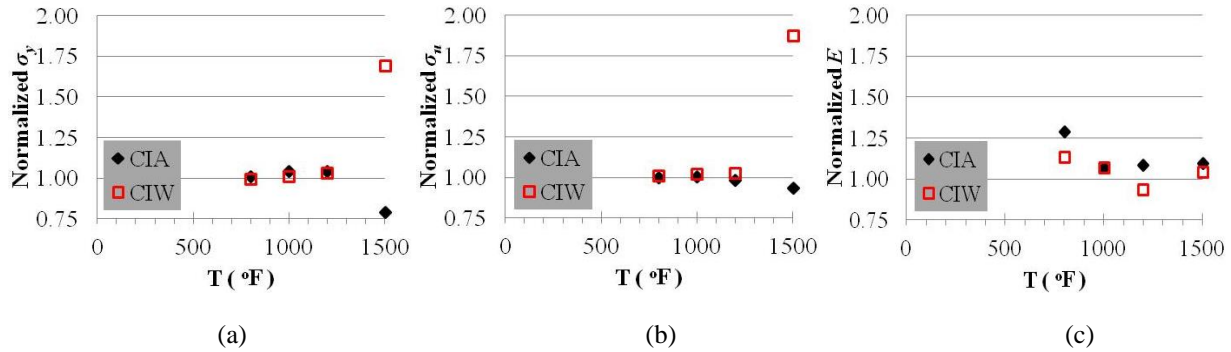


**Figure 24.** Normalized plots of average values of (a)  $\sigma_y$ , (b)  $\sigma_u$  and (c)  $E$  for A588 steel specimens that were heated to the temperature specified on the x-axis and cooled in air (CIA) or cooled in water (CIW). The normalization is based on the average ‘control’ value from the specimens that were not heated.

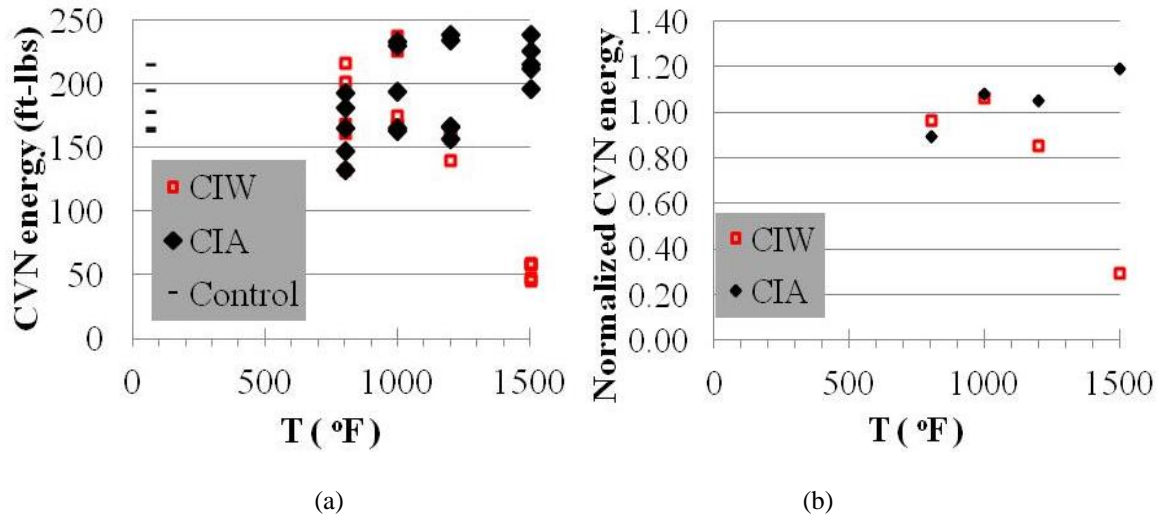
## 5.4. Fracture Toughness

Table 7 summarizes the CVN test results that measure fracture toughness. Figures 25a and 26a plot the CVN energy (ft-lbs) for specimens with Material 1 and 2 (A588), respectively. Figures 25b and 26b plot the CVN results normalized by the control CVN specimens (those that were neither heated nor cooled). The results from Figure 25 show that for Material 1, the CVN specimens that were heated to 800°F and 1000°F, the CVN values remain about the same regardless if the specimen is CIA or CIW. For the CVN specimens heated to 1200°F, the CIW specimens tend to have lower CVN energy than the CIA specimens. For CVN specimens heated to 1500°F, the CIA specimens have slightly higher CVN energy compared to the control, while the CIW specimens show a dramatic reduction.

Figure 26 shows that for specimens with A588 steel and heated to 800°F, 1000°F, and 1200°F, the CVN energies remained approximately the same regardless of whether the specimen was CIA or CIW. For the specimens that were heated to 1500°F, the CIA specimen average remained close to the control, but the CIW specimens showed a significant drop in their CVN energies compared to the control specimens.

**Table 7.** Summary of residual fracture toughness (CVN) results.

	Material 1			Material 2 (A588)		
	Spec.	CVN (ft-lb)		Spec.	CVN (ft-lb)	
		avg.	std. dev.		avg.	std. dev.
	<b>1A</b>	<b>183</b>	<b>20</b>	<b>2A</b>	<b>125</b>	<b>10</b>
CIA	1Ca-800	164	24	2Ca-800	143	37
	1Ca-1000	198	35	2Ca-1000	133	36
	1Ca-1200	193	41	2Ca-1200	156	18
	1Ca-1500	218	16	2Ca-1500	127	38
CIW	1Cw-800	177	33	2Cw-800	132	21
	1Cw-1000	195	34	2Cw-1000	127	25
	1Cw-1200	156	10	2Cw-1200	150	26
	1Cw-1500	54	6	2Cw-1500	9	1



**Figure 25.** Residual CVN energy for Material 1 specimens that were heated to the specified maximum temperature and cooled in water (CIW) or cooled in air (CIA): (a) Results from all tests for each temperature and cooling method, (b) CVN values normalized by the average ‘control’ value (specimens that were not heated).

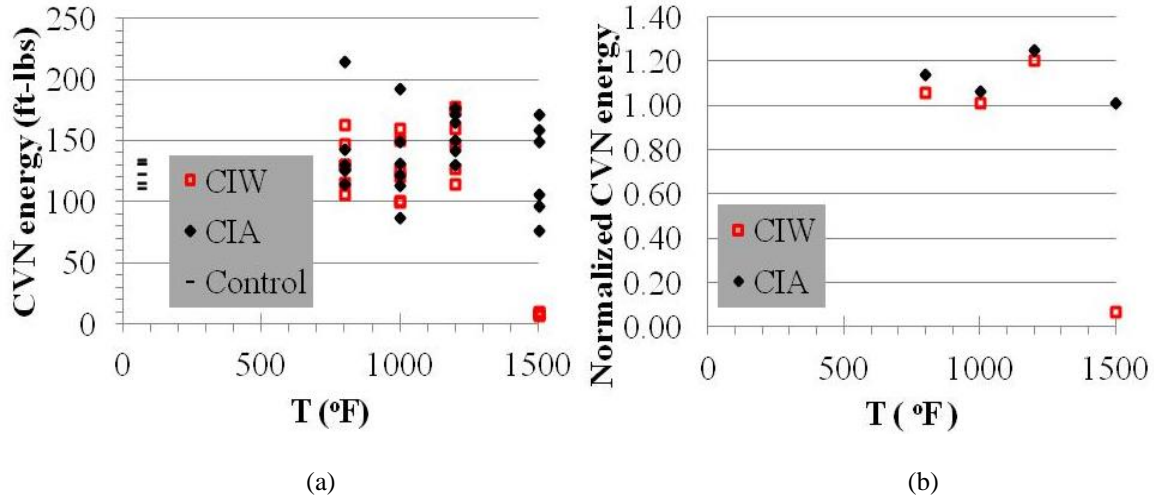


**Figure 26.** Residual CVN energy for A588 specimens that were heated to the specified maximum temperature and cooled in water (CIW) or cooled in air (CIA): (a) Results from all tests for each temperature and cooling method, (b) CVN values normalized by the average ‘control’ value (specimens that were not heated).

## 5.5. Hardness

Table 8 presents the average hardness values and the standard deviation. For both materials, cooling method, and maximum temperature of heating, three CVN specimens were selected randomly and three hardness measurements taken on each. Therefore, each of the values in Table 8 is the average of 9 measured values of hardness. The hardness test results are presented in the HRB scale. However, specimen 2C<sub>w</sub>-1500 had a hardness that exceeded the range measurable accurately with the Rockwell Hardness B-Scale. Using the B Scale, readings above 100 may be inaccurate due to blunt shape of ball indenter and the danger of ball flattening under high pressure of the load. In these cases, the next heavier load or smaller penetrator should be used [Wilson Instruments].

Since we were already using the largest test force for HRB (100 kgf) and smallest indenter (1/16” diam), we conducted this test with HRC and converted the value to the B-Scale readings per ASTM E140-12b. For example, the initial (average) reading in the HRB scale indicated a value of 104.5. Using the HRC scale, the average reading for 2C<sub>w</sub>-1500 was 28.5, which was converted according to ASTM E140-12b for high-nickel alloys. The result of the conversion into HRB scale reading was 104, indicating the initial reading was accurate enough.

Figures 27 and 28 plot the hardness values measured for Material 1 and A588, respectively. It is observed that the CIA specimens, for both materials, retain their hardness values (essentially unaffected). For the CIW specimens, however, a clear trend is observed where the larger the temperature, the larger the residual hardness.

**Table 8.** Summary of residual Rockwell Hardness tests.

	Material 1			Material 2 (A588)		
	Spec.	hardness (HRB) avg.	std. dev.	Spec.	hardness (HRB) avg.	std. dev.
	1A	80.7	0.6	2A	86.1	0.4
CIA	1Ca-800	80.8	0.5	2Ca-800	87.0	0.6
	1Ca-1000	80.3	0.8	2Ca-1000	87.9	0.8
	1Ca-1200	80.6	0.6	2Ca-1200	88	0.8
	1Ca-1500	79.1	1.5	2Ca-1500	88.9	1.5
CIW	1Cw-800	81.5	1.1	2Cw-800	88.4	0.6
	1Cw-1000	83.5	1.0	2Cw-1000	89.8	0.5
	1Cw-1200	86.2	0.9	2Cw-1200	91.3	1.1
	1Cw-1500	92.4	1.1	2Cw-1500	*104	1.0

\*Converted value from HRC to HRB scales.

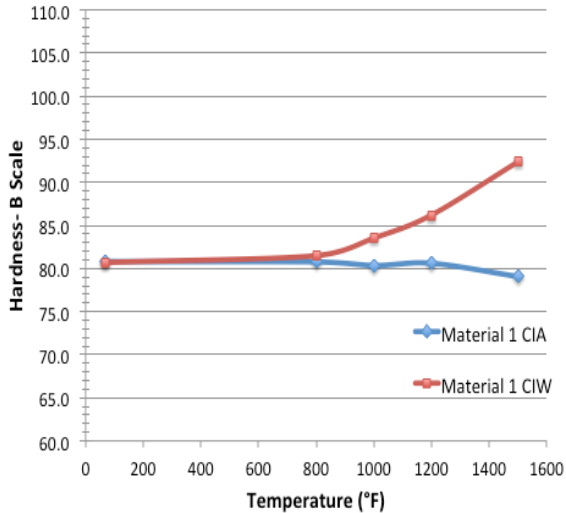


**Figure 27.** Residual Rockwell hardness results for Material 1.

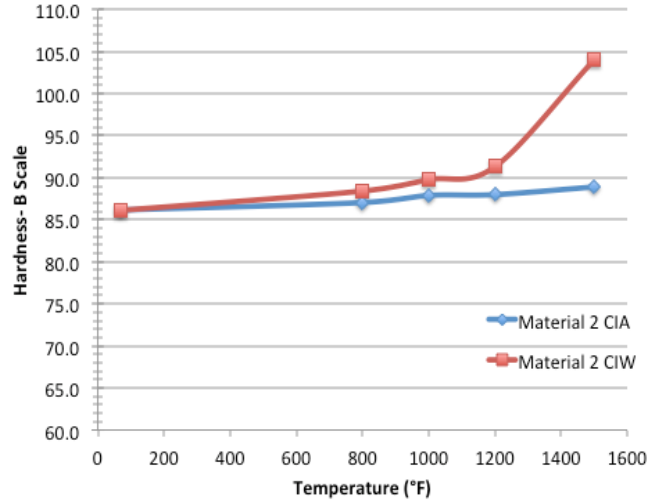


**Figure 28.** Residual Rockwell hardness results for Material 2 (A588)

## 6.0. CONCLUSIONS

The mechanical properties of A588 weathering steel that has been exposed to high temperatures was studied in comparison to another material ('Material 1') whose chemical composition and mechanical properties allowed it to be classified by ASTM as both an older weathering steel (A242), a steel commonly used in building construction (A992), and also A709 Grade 50, a non-weathering steel used for bridges. The properties studied include the residual (after heating and cooling) stress-strain, fracture toughness, and surface hardness. In addition to material type, other parameters studied were temperature (427° C (800° F), 538° C (1000° F), 649° C (1200° F), and 815° C (1500° F)) and cooling methodologies (cooling in air (CIA), and cooling in water (CIW)). The CIW method represents firefighting effects

### 6.1. Effect of Temperature on Tensile Capacity

The general trend observed for both materials is consistent with what is expected for steel at elevated temperatures: with increasing temperature there is reduced stiffness, reduced ultimate strength, and increased ductility. However, there were some unexpected behaviors. For example, for both materials, the ultimate strain for the tests at 1000°F decreased compared to the 800°F tests.

### 6.2. Effect of Cooling Method on Residual Mechanical Properties

The two cooling methods studied, cool in air (CIA) and cool in water (CIW), were selected to reflect actual bridge fire situations. The two methods reflect two firefighting measures: do not point the hose at the bridge and let it cool slowly, or use water to fight the fire and cool the bridge quickly. The following summarizes the results:

- For both materials, the CIW and CIA specimens heated to 800°F, 1000°F, and 1200°F resulted in no significant change in  $\sigma_u$  or  $\sigma_y$  or E.
- For specimens heated to 1500°F and cooled in water, a noticeable change in  $\sigma_y$  was observed: 16% increase for Material 1, and 69% increase for A588.
- For specimens heated to 1500°F and cooled in water, a noticeable change in  $\sigma_u$  was observed: 58% increase for Material 1, and 88% increase for A588.
- The specimens heated to 1500°F and cooled in water (CIW) failed in a brittle mode with almost no necking in the specimen.
- The modulus of elasticity did not seem to be affected by the method of cooling.
- There did not appear to be a significant effect on CVN results for the CIA specimens. However for the CIW specimens, there is a clear trend of decrease in fracture toughness with increase in temperature. For example, for Material 1, the CVN value drops from 183 ft-lb for the unheated specimen to 54 ft-lb for the specimen heated to 1500°F and cooled in water (CIW). For A588, the CVN value drops from 125 ft-lb for the unheated specimen to 9 ft-lb for the specimen heated to 1500°F and cooled in water (CIW).
- When heated and cooled slowly by air (CIA), both materials seem to maintain a relatively constant hardness. However, when cooled rapidly by water (CIW), a clear increase in hardness is observed with increasing temperature.

### 6.3. Comparison of Materials

The following summarizes the comparison of the two materials tested:

- At ambient temperature, the A588 steel has a larger  $\sigma_u$ , similar  $\sigma_y$ , smaller fracture toughness, and slightly larger hardness than Material 1.
- At elevated temperatures, the A588 steel  $\sigma_u$  decreases faster with increasing temperatures and is more ductile for temperatures less than 1000°F compared to Material 1.
- The A588 steel seems to be affected more than Material 1 in terms of residual strength at 1500°F. At other temperatures there is not a significant effect on either material.
- A588 steel has lower fracture toughness values than Material 1
- A588 steel has larger hardness values than Material 1

### 7.0. RECOMMENDATIONS

The studies showed that at temperatures of 1200°F and below, the residual material properties of both materials studied (representing the post-fire condition), were affected no more than on the order of 10% compared to the unheated steel. However, specimens tested to 1500°F showed a significant change in response, especially for the cool in water (CIW) method of cooling. At this temperature, the steel has likely gone through a phase change. More studies are needed to evaluate the microstructure changes that happen in this steel when it has been heated to 1500°F and then cooled in air or water.

Practically speaking, however, a bridge that reaches 1500°F will experience significant permanent deformations if this temperature is widespread and in that case it may need to be demolished. Therefore, it is likely that if significant permanent deflections are not observed, a bridge of A588 weathering steel could potentially be put back into service following a fire since below this temperature, significant changes in material properties are not observed once the steel has cooled.

A588 steel has lower fracture toughness and higher hardness than Material 1. Furthermore, for the CIW specimens, there is a clear trend of decreasing fracture toughness with increasing temperature. There is also a clear trend of increasing hardness with increasing temperature. It is expected that the CIW method produces different microstructure changes than the CIA method, thus resulting in the trends observed. But if temperatures are 1200°F and below, these changes are not significant.

This study has characterized high temperature properties of a common weathering steel used in bridges. The study has identified that further work is needed in evaluating microstructural changes at elevated temperatures and with different cooling methods. In addition, ongoing work is examining the effect of the patina on the thermal response.

## 8.0. REFERENCES

- American Iron and Steel Institute (1995). *Performance of Weathering Steel in Highway Bridges*, A Third Phase Report.
- ASTM (2013). Standard Specification for Structural Steel for Bridges, **ASTM A709**, American Society for Testing and Materials, West Conshohocken, PA.
- ASTM (2013). Standard Hardness Conversion Tables for Metals, ASTM E140-12b, American Society for Testing and Materials, West Conshohocken, PA.
- ASTM (1979). Standard Specification for High-Strength Low-Alloy Structural Steel, **ASTM A242**, American Society for Testing and Materials, West Conshohocken, PA.
- ASTM (2010). Standard Specification for High-Strength Low-Alloy Structural Steel, up to 50 ksi [345MPa] Minimum Yield Point, with Atmospheric Corrosion Resistance, **ASTM A588**, American Society for Testing and Materials, West Conshohocken, PA.
- ASTM (2011). Standard Specification for Standard Specification for Structural Steel Shapes, **ASTM A992**, American Society for Testing and Materials, West Conshohocken, PA.
- ASTM (2009). Standard Test Methods for Tension Testing of Metallic Materials, **ASTM E8**, American Society for Testing and Materials, West Conshohocken, PA.
- ASTM (2008). Standard Test Methods for Rockwell Hardness of Metallic Materials, **ASTM E18**, American Society for Testing and Materials, West Conshohocken, PA.
- ASTM (2000). Standard Test Methods for Notched Bar Impact Testing of Metallic Materials, **ASTM E28**, American Society for Testing and Materials, West Conshohocken, PA.
- CAIT (2013). “On call, on site, and on the case: New CAIT bridge program supports NJDOT as the care for our state’s bridges” CAIT Newsletter, Issue 11, January.
- European Committee for Standardization (CEN) (2002). Eurocode 1: Actions on Structures - Part 1-2: General Actions - Actions on Structures Exposed to Fire. Brussels.
- Garlock, M., Payá-Zaforteza, I. Kodur, V., Gu, L., (2012). “Fire Hazard in Bridges: Review, Assessment and Repair Strategies”, *Engineering Structures*, Elsevier, V. 35, p. 89-98.
- Kimura, M., Kihira, H., (2005). “Nanoscopic Mechanism of Protective Rust Formation on Weathering Steel Surfaces”, Nippon Steel Technical Report
- Lie, T.T. (1992). *Structural Fire Protection: Manual of Practice*. ASCE Manuals and Reports of Engineering Practice. No. 78. American Society of Civil Engineers.
- Luecke, W.E., Banovic, S. and McColskey, J.D. (2011). “High-Temperature Tensile Constitutive Data and Models for Structural Steels in Fire”. *NIST Technical Note 1714*. U.S. Department of Commerce. National Institute of Standards and Technology. November.

McDad, B., Laffrey, D.C., Dammann, M., Medlock, R.D., (2000). Performance of Weathering Steel in TxDOT Bridges, Texas Department of Transportation.

New York State Department of Transportation (2008). Bridge Fire Incidents in New York State (Private Correspondence with Prof. M. Garlock), New York State Department of Transportation, USA.

NJDOT (2010). "Bridge re-evaluation survey report: Structure No. 1135-150 I-195 Eastbound over NJ Turnpike" Sept. 1.

Payá-Zaforteza, I, Garlock, M. (2012). "A numerical investigation on the fire response of a steel girder bridge", Journal of Constructional Steel Research, Elsevier, V. 75, p.93-103.

PennDOT (2011). "Effects of Fire Damage on the Structural Properties of Steel Bridge Elements", PennDOT, April 30.

US Department of Transportation, FHWA (2012). Bridge Steels and Their Mechanical Properties, FHWA-IF-12-052.

Wiss, Janney, Elstner Associates, Inc. (2013). Assessment of Weathering Steel Bridge Performance in Iowa and Development of Inspection and Maintenance Techniques, Iowa DOT.

Wilson Instruments, Instron Company "Fundamental of Hardwell Rockness Testing"